Data Descriptor

Taguchi Orthogonal Array Dataset for the Effect of Water Chemistry on Aggregation of ZnO Nanoparticles

Rizwan Khan[1], Muhammad Ali Inam[1], Du Ri Park[1], Saba Zam Zam[1] and Ick Tae Yeom[1,] *

[1]Graduate School of Water Resources, Sungkyunkwan University (SKKU) 2066, Suwon 16419, Korea; rizwankhan@skku.edu (R.K.); aliinam@skku.edu (M.A.I.); enfl8709@skku.edu (D.R.P.); sabazamzam@skku.edu (S.Z.Z.)

*Correspondence: yeom@skku.edu; Tel.: +82-31-299-6699

Abstract: The extensive use of engineered nanoparticles (ENPs) such as zinc oxide nanoparticles (ZnO NPs) in various commercial fields has spurred significant concern about its possible toxicological effects of ZnO NPs on human health and eco-system. Therefore, it is substantial to understand the aggregation phenomena which could attenuate this effect. This data article provides information on aggregation of ZnO NPs under the influence of various parameters of water chemistry. Moreover, Taguchi orthogonal array $L_{27}(3^{13})$ design matrix was used to evaluate the effect of multiple parameters in aqueous solution. The data were obtained from single beam UV-Vis spectrophotometer (Optizen 2120 UV, Mecasys, Korea) using Optizenview 4.2.5 PC interference software, Fourier transform infrared spectrometer (FT/IR-4700, spectroscopy, JASCO Analytical Instruments, Easton, USA) and particle electrophoresis (NanoZS, Zetasizer, Malvern Instruments Ltd, Worcestershire, UK). The dataset draws attention on dominant parameters influencing aggregation of ZnO NPs in water. The analysis of variance (ANOVA) data revealed that electrolyte concentration, type and natural organic matter (NOM) concentration were the most significant parameters. Furthermore, FT-IR data presents a possible mechanism of ZnO NPs stabilization in the presence of different NOM. This data will be helpful for the development of environmental risk assessment strategies and prediction of fate and mobility of other ENPs in the aquatic environment.

Dataset: Available as the supplementary file.

Dataset License: CC-BY

Keywords: aggregation; Fourier transform infrared spectrometer; particle electrophoresis; risk assessment; Taguchi orthogonal array; UV-Vis spectrophotometer; zinc oxide nanoparticles

1. Summary

With the development of nanotechnology, production and utilization of engineered nanoparticles (ENPs) increase in consumer products and commercial applications. Among diverse ENPs, zinc oxide nanoparticles (ZnO NPs) is third largest used metal-containing nanomaterials due to its unique structural properties [1]. The estimated annual global production was between 570-33,400 tons/year, which anticipated to be 58,000 tons/year by 2020 [2]. However, such broad applications and production of ZnO NPs have generated concern to both scientific and public community due to its environmental release, that may increase the bioavailability and NPs toxicity in an aqueous environment [3]. The potential adverse effects of ZnO NPs on phytoplankton, plants, mammals, and even human cell lines are well known [4]. However, the limited knowledge is available on the nanoparticle-liquid interaction and aggregation among NPs. Thus, understanding the aggregation phenomena of ZnO NPs under various parameters of water chemistry is important to properly assess their risk.

Several researchers have studied the ZnO NPs fate and mobility in an aqueous environment [5–7]. The ZnO NPs aggregation phenomena are highly influenced by physicochemical properties and solution chemistry [8]. The NPs properties such as size, shape and coating may cause substantial variation in its aggregation kinetics [9]. Few studies [10,11] reported that large size particles tend to aggregate, however, tiny size particles remain suspended in the solution and increase the risk to aquatic species. The variation in solution pH and temperature affect the surface potential and solubility of ZnO NPs which may also influence its agglomeration phenomena [7,12]. The fast aggregation reported in high salt content solution due to compression of the electrical double layer (EDL) [9,13]. The ubiquities natural organic matters (NOM) stabilizers kept ZnO NPs suspended in water due to steric hindrance and potential charge reversal [14,15]. Furthermore, few studies demonstrated that the presence of divalent cations i.e. Ca^{2+}, Mg^{2+} may form intermolecular bridging between NOM and ZnO NPs, thus enhance the hetero-aggregation [16]. In the previous studies [17–20], the influence of various environmental parameters on agglomeration phenomena of ZnO NPs has generally studied by some individual factors and limited to pure water. Additionally, the interaction of multiple parameters affecting this phenomenon has been rarely touched by environmental scholars. Therefore, it is important to evaluate the aggregation phenomena of ZnO NPs together with a combination of different parameters, consequently, that may affect the fate and toxicity in the ecosystem.

A recent study has shown a significant influence of several environmental parameters on sedimentation and aggregation of ZnO NPs [21]. Although, numerous dataset on such phenomena of other ENPs i.e. copper oxide (CuO) and titanium dioxide (TiO_2) have been reported [19,22]. However, to the knowledge of the authors, there are no datasets available on the effect of combined multiple environmental parameters on ZnO NPs aggregation. In light of this, ZnO NPs aggregation phenomena in single and multiple environmental parameters were investigated. The fractional factorial method based on Taguchi orthogonal array (OA) L_{27} (3^{13}) design matrix was used to measure the main and interactive effect of multiple factors. This study quantitatively presents the ZnO NPs aggregation dataset obtained from UV-Vis spectrophotometer, Fourier transform infrared spectrometer (FT-IR), and zeta potential analyzer and Optizen view 4.2.5 PC interference software.

The dataset obtained from UV/Vis spectrophotometer presents the absorbance data of ZnO NPs at various environmental conditions such as pH, electrolyte type and concentration, and NOM type and concentration. Earlier, the zeta potential and FT-IR spectra of ZnO-NOM complexes were elucidated under different aqueous matrices [21]. This data may contribute to better understand the agglomeration phenomena and fate of ZnO NPs in the complex heterogeneous environment.

2. Data Description

Here, we present the dataset of ZnO NPs aggregation efficiency and its kinetics in an Excel (Microsoft Corp., Redmond, WA) spreadsheet file. Table S1-S12 show the ZnO NPs data obtained after bench scale aggregation experiment which are listed and described in Table 1-2 at 25°C±0.5. Table S1-S2 show the absorbance data across various wavelength and concentrations. This data is used to determine the concentration from quantitative standard linear curve based on Beers-Lambert law. Table S3 shows turbidity data at various time and power levels of sonicator to obtain the optimum sonication condition for further aggregation experiments. The data in Table S4-S6 shows the residual absorbance and corresponding zeta potential at various pH, electrolyte, NOM types and concentrations after 6 hours. This can be used to predict the effect of interfering ions on the aggregation phenomena of ZnO NPs in aqueous environment. Table S7 shows the time-resolved optical absorbance measured at 370 nm across various solution matrices. The aggregation rate k can be estimated from this data using Stokes sedimentation theory, it also indicates that aggregation kinetics may vary substantially in the presence of high electrolyte and NOM concentrations. The Table S8 shows the data derived from FT/IR spectra of pristine ZnO NPs before and after interaction with high concentration of various NOM i.e. humic acid, salicylic acid and citric acid. It shows the percent transmittance against the wave numbers (500-4000 cm^{-1}). This data is helpful in providing the information about modification in the surface of ZnO NPs after interaction with NOM.

Furthermore, the Table S9-S11 shows the data of residual absorbance and corresponding aggregation efficiencies, variance and range analysis obtained from Taguchi OA L_{27} (3^{13}) matrix for multi-parameters experiments. This data is important to determine the analysis of variance (ANOVA) and consequently the dominant parameter influencing the ZnO NPs aggregation in a real environment. In addition, the data in Table S12-S13 shows the residual absorbance and aggregation efficiencies obtained across various environmental tested waters. This data is helpful in providing ZnO NPs aggregation phenomena in the real environmental conditions.

Table 1. Type of experiment and condition of single parameter experiments

Experiment	Parameter	Unit	Condition
A	pH	-	3 to 12
B	KCl, Na_2SO_4	mM	0.01 to 100
	$MgCl_2$	mM	0.01 to 25
C	HA, SA, CA	mgL^{-1}	0.5 to 100
D	Synthetic Environmental water samples		

Where HA, SA and CA corresponds to humic acid, salicylic acid and citric acid respectively

Table 2. Parameter and their corresponding levels of the Taguchi (OA) experiment

Parameter	Units	Level		
		1	2	3
pH	-	7.0	8.0	9.5
Electrolyte Concentration	mM	25	50	100
NOM Concentration	mgL^{-1}	5	10	25
Electrolyte type	-	KCl	Na_2SO_4	$MgCl_2$
NOM type	-	HA	SA	CA
Temperature	˚C	15	25	35

Where NOM corresponds to natural organic matter

3. Methods

3.1. *Solution and synthetic waters preparation*

The nanopowder of ZnO NPs assay 97%; humic acid (HA), salicylic acid (SA) and citric acid (CA) were purchased from the Sigma-Aldrich (St. Louis, MO, USA) and used without further purification. While inorganic salts i.e. potassium chloride (KCl), sodium sulfate (Na_2SO_4), magnesium chloride ($MgCl_2.6H_2O$), nitric acid (HNO_3), hydrochloric acid (HCl), sodium hydroxide (NaOH) used in this study were obtained from local suppliers. According to the vendor, NPs have particle size <50 nm with a specific surface area 15-25 m^2/g and it contain 6% Al as dopant. The 100 mg/L of ZnO NPs solution was prepared by adding 12.57 mg of ZnO nanopowder in 100 ml of nanopure water. The solution was subjected to sonicate from 5-40 min and 100-600W power to obtain a homogenous NPs dispersion. Moreover, the solution turbidity was also measured using Turbidimeter (Hach Benchtop 2100N, Loveland, CO, USA). The natural organic matter (NOM) stock solutions were prepared by dissolving 1g powder of each NOM in 1L of deionized (DI) water. The pH of HA was adjusted to 10 using NaOH to ensure complete dissolution of HA. The solution was stirred at 600 rpm for overnight to improve further stability [23]. All the stock solutions pH were adjusted to 7 prior to storage in dark at 4°C. The stock solutions of inorganic salts with 1 M ionic strength were prepared by adding 7.45g KCl, 14.2g Na_2SO_4 and 20.32g $MgCl_2.6H2O$ in 1L solution respectively. Four synthetic waters were prepared in the laboratory, while tapwater and wastewater were collected from Sungkyunkwan University, Suwon and metal processing industry located at Ulsan, Korea respectively. The detailed characteristics of all water samples are already presented in our previous study [21]. The IS (Ie) was calculated from the electrical conductively (EC) according to the following equation.

$$Ie = 0.01442 \times EC^{1.009} \tag{1}$$

3.2. Standard calibration curve analysis

Prior to aggregation experiments, the optical absorption analysis was conducted on the UV/Vis spectrophotometer (Optizen 2120 UV, Mecasys, Korea) using a 100 mm path length quartz cuvette. The device is equipped with high-quality Tungsten-Halogen lamp and a Deuterium lamp which allows the analysis of ZnO NPs at relatively low concentrations (100 to 1000 µg/L). The absorption spectra of the colloids were collected between 200-800 nm at 25 °C. The background was set up with the proper solvent and then, each colloid sample was examined. Since UV-Vis spectra fit well to Beers-Lamber law, thus a standard calibration curve was collected at 370 nm and used as a quantitative criterion of ZnO NPs. The ZnO NPs concentration and aggregation efficiency was estimated using fitted curve equation having R^2 of 0.9993 as shown in equation 2 and 3. In current study, initial concentration of ZnO NPs in vial was maintained at 100 mg/L.

$$Y = 0.0086x - 0.0116 \tag{2}$$

Where Y represents the concentration of ZnO NPs and x indicates residual absorbance.

$$A = \frac{Ci - Ct}{Ci} \times 100 \tag{3}$$

Where A corresponds to aggregation efficiency, Ci and Ct are concentration of ZnO NPs before and after aggregation experiments.

3.3. Control experiments

The experiments were conducted in standard sedimentation glass tube (Fisher Scientific Co., Fair Lawn, NJ) with the dimensions (height; 30cm, radius; 2cm) for 6 hours. The predetermined concentration of inorganic salts and NOM were spiked into 100mg /L of ZnO NPs suspension. The pH was adjusted using 0.1 M HCl and 0.1 M NaOH solution. The suspension was subjected to ultrasonication to fully disperse the NPs in solution. After completion of aggregation experiments, 1ml aliquot were collected from each suspension tube at ¼ height to measure the absorbance of residual ZnO NPs. Prior to aliquot analysis, equipment was calibrated using a blank nanopure water solution. Following this approach, single and multiple parameter experiments were performed as shown in Table 1-2. In the case of kinetic experiments, the instrument was specifically tuned in UV/Vis kinetic mode to optimize the wavelength at 370 nm and time setting in the selection window. Afterward the sample was placed in a quartz cuvette and the absorbance was continuously measured after every 3 min of the time interval. The settling rate and velocity of the NPs were calculated using first-order kinetics and Stokes's equation [24] respectively.

$$\ln Ct = \ln Ci - kt \tag{4}$$

Where t represents the time; C_i and Ct are ZnO NPs concentrations at initial and t time points, respectively; and k is the sedimentation rate in (h^{-1}).

$$V_t = \frac{gd^2(\rho_\rho - \rho_m)}{18\mu} \tag{5}$$

Where g represents acceleration of gravity (m/s^2), d particle diameter (m), ρ_ρ density of particle (g/cm^3), ρ_m density of medium (g/cm^3), μ viscosity of medium (g/m.s) and Vt settling velocity of particles respectively.

3.4. Sample preparation for FTIR measurement

The Fourier transform infrared spectra (FT/IR-4700, spectroscopy, JASCO Analytical Instruments, Easton, USA) of ZnO NPs before and after interaction with various NOM were recorded. The spectroscopy has been used as a useful tool for identification of structures and functional groups. The extracted aliquots of ZnO NOM complexes after aggregation experiment were collected and NPs were separated by centrifugation (Hettich Centrifuger Universal 320R, Germany) at 3000 RPM for 15 min. The resultant ZnO NPs pellets were subjected to vacuum drying for 24 hours to remove any moisture content. The high sensitive Mercury–Cadmium–Telluride (MCT) focal-plane array detector was cooled for 30 min with liquid nitrogen (LIN). The dried samples were inserted into the sample platform to characterize the attachment of functional groups in the range of wave number 500-4000 cm^{-1}. The Thermo Scientific OMNIC FTIR software was used to analyze the data and exported in the text file format for further processing.

3.5. Zeta potential analysis

After the aggregation experiments, an aliquot was removed from the suspension and placed into the zeta potential cell. The cell was filled up with the colloids avoiding the presence of bubbles. The electrophoretic mobility of the particles was measured using a Zetasizer Nano-ZS (Malvern Instrument). The temperature in the Zetasizer was set to 25 ± 0.1 ºC. Three electrophoretic mobility measurements were made for each sample. The value of electrophoretic mobility was directly converted by default function of equipment. The default Smoluchowski equation is given [25] below .

$$\zeta = 4\pi\eta \left(\frac{V}{E}\right)/\varepsilon \qquad (6)$$

Where ζ represents zeta potential (mV), $\left(\frac{V}{E}\right)$ electrophoretic mobility (microns /sec x volt/cm), η solvent viscosity (poise) and ε is dielectric constant.

3.4 Elemental analysis

The aliquot obtained from tap and industrial wastewater were filtered through 0.45 um glass fiber filter; digested with 99% pure HNO3 prior to analysis [26]. The Inductively coupled plasma mass spectrometry (ICP-MS, 7700x, Agilent Technologies, Palo Alto, CA, USA) was used to analyze the concentration of common element. The industrial wastewater filtered samples were further diluted in 1:10 ratio to measure concentration of common anions (NO_3^-, Cl^- and SO_4^{-2}) using ion chromatography with metrosep A Supp5 column in (861 Advanced Compact IC, Metrohm, Herisau, Switzerland).

3.5 Taguchi Orthogonal array experimental design

In recent years, Taguchi method developed by Dr. Genichi Taguchi has been used widely in engineering fields to optimize and design experiments [27,28] . The Taguchi fractional factorial design utilized the orthogonal array (OA) design matrix theory to study large number of variables with small number of experimental trials. In present study, it was planned to investigate the ZnO NPs *aggregation phenomena* under the control of six parameters i.e. A, B, C, D, E and F with three levels and two potential interactions i.e. AxB and BxC. The standard linear graph was modified using the line separation method as shown in Figure 1, to assign the parameters and interactions to various columns of OA. The OA chosen was $L_{27}(3^{13})$ which has 27 rows corresponds to number of experiments with 13 columns at 3 levels as shown in Table S9. The plan of experiment was as follows. The pH (A) was assigned in first column, electrolyte concentration (B) in second column, NOM concentration (C) in fifth column, electrolyte type (D) in ninth column, NOM type (E) in tenth column and temperature (F) in twelfth column. The possible two parameter interactions $(AxB)_1$ and $(AxB)_2$ were assigned to third and fourth columns while eighth and eleventh were assigned to $(BxC)_1$ and $(BxC)_2$ interactions. The remaining sixth, seventh and thirteenth columns were left empty in order to calibrate the standard matrix. The experiments were conducted for each combination of parameters as per selected OA in triplicate and average values were reported.

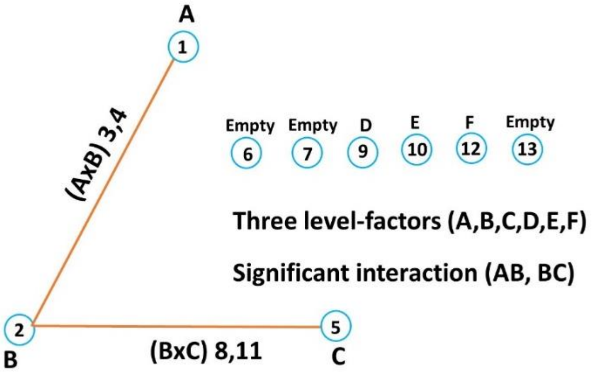

Figure 1. Modified linear L_{27} (3^{13}) graph and column assignment

3.5. Statistical Analysis

The experimental data obtained by following the Taguchi OA matrix procedure were analyzed by the general linear model (GLM) with Tukey's post Hoc test using the software MINITAB18.0 (Six Sigma Academy International). The MINITAB was also used for range analysis and analysis of variance (ANOVA) and predicting the dominant parameters for ZnO NPs aggregation. Probability p-value less than 0.05 were considered to be significant. The normality and homogeneity of data were considered before conducting the ANOVA. Each experiment was performed in triplicate and average values were reported.

3.6. Optizen view 4.2.5

A UV-Vis spectrophotometer was connected with a PC interference software "Optizen view 4.2.5" to obtain the absorbance and real-time kinetics data of ZnO NPs in solution. The method adopted for obtaining sample survey scan and kinetic data is illustrated in Figure 2(a-d).

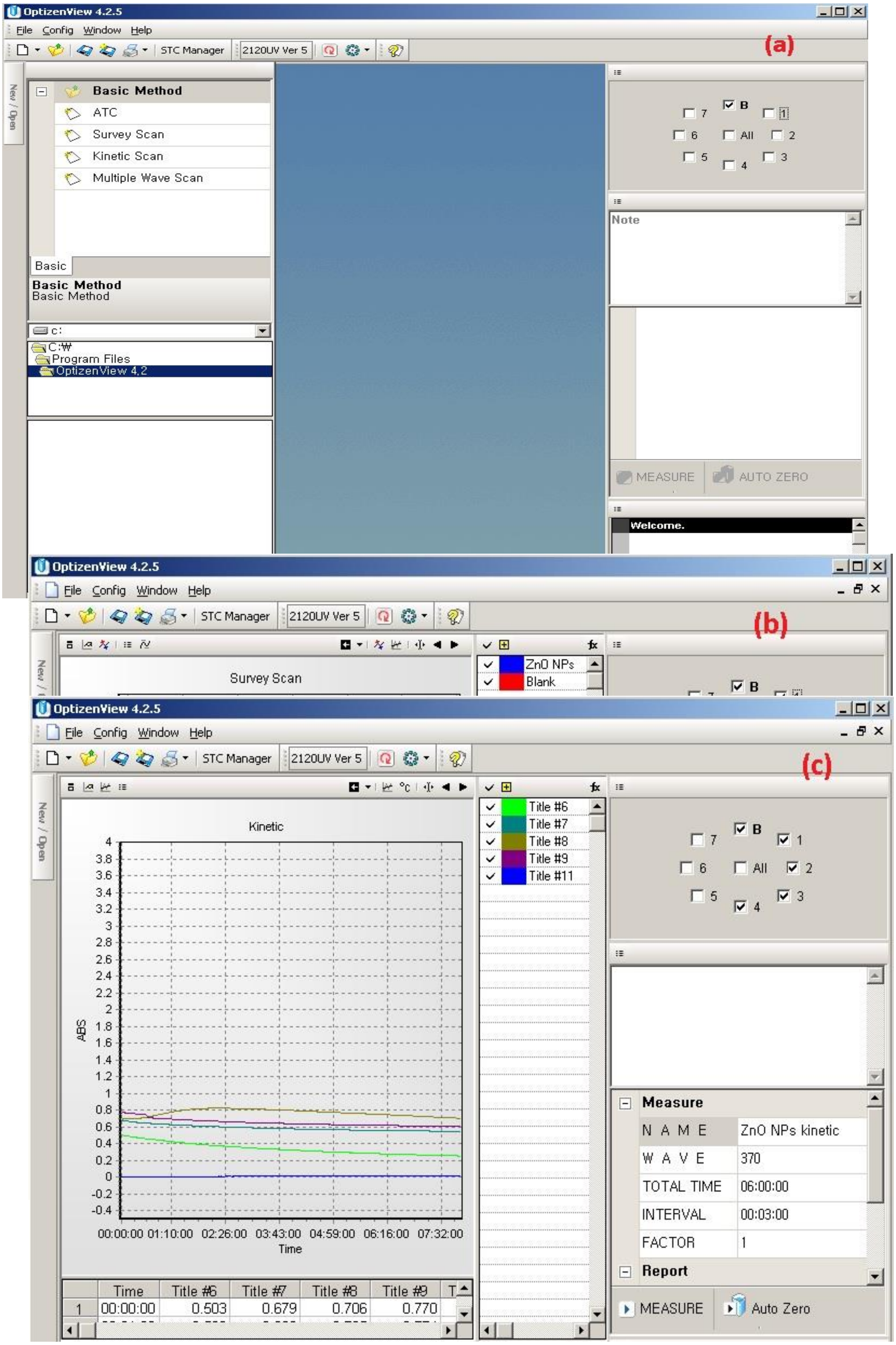

Measure

NAME	ZnO NPs kinetic
WAVE	370
TOTAL TIME	06:00:00
INTERVAL	00:03:00
FACTOR	1

Report

	Time	Title #6	Title #7	Title #8	Title #9
1	00:00:00	0.503	0.679	0.706	0.770

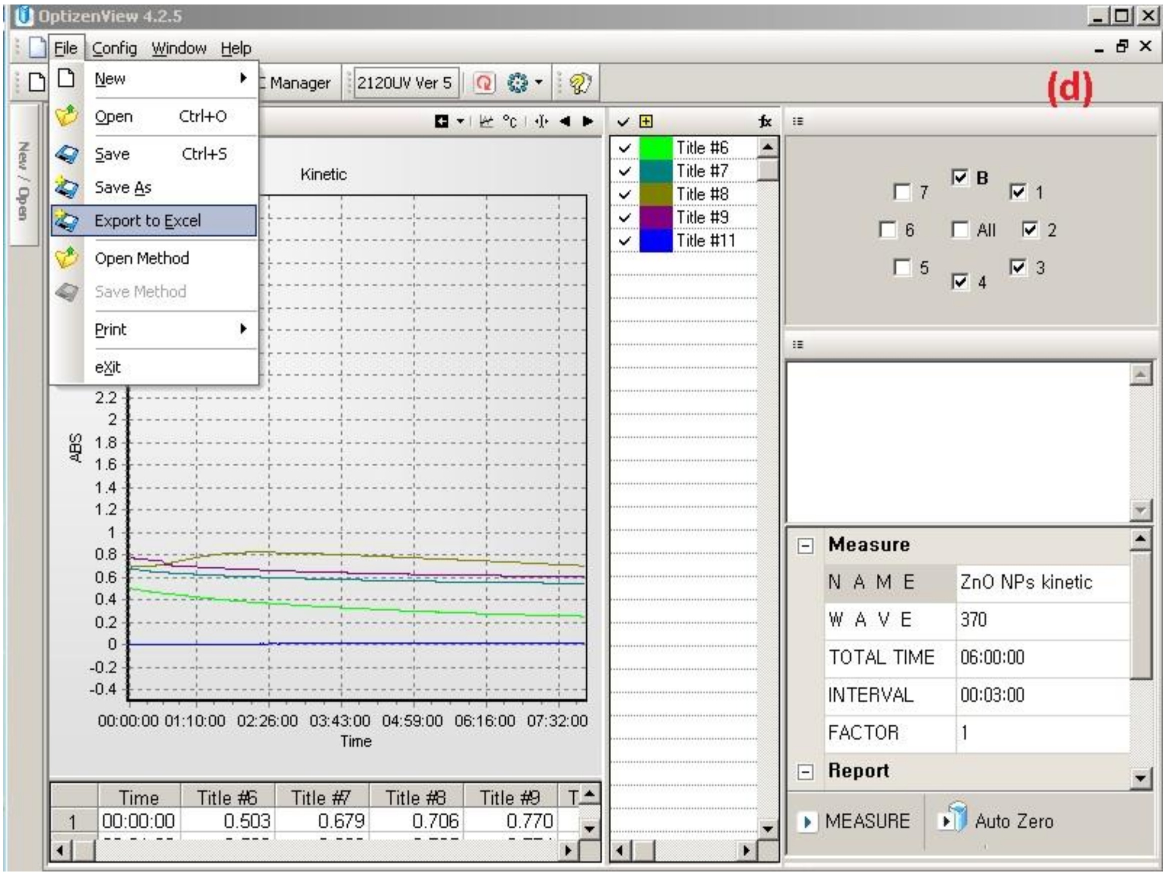

N A M E	ZnO NPs kinetic
W A V E	370
TOTAL TIME	06:00:00
INTERVAL	00:03:00
FACTOR	1

	Time	Title #6	Title #7	Title #8	Title #9	T
1	00:00:00	0.503	0.679	0.706	0.770	

Figure 2. An illustration of Optizen view with survey scan and kinetic study data.

4. User note

Our dataset provides quality information about the sedimentation and aggregation phenomena of ZnO NPs that might be useful for researchers and scientific community. The approach described here may help researchers who intend to increase the number of parameters and their interactions, in the range of our dataset. In addition, it may add to toxicological studies about ENPs, given that many parameters in our dataset are commonly found in natural water bodies. In the view of global scale, one may use the dataset to incorporate more information of water chemistry parameters present in the local environments to assess other parameters that were not covered in current matrix data.

Supplementary Materials: The following are available online at www.mdpi.com/xxx/s1, Figure S1: title, Table S1: title, Video S1: title.

Author Contributions: R.K. and I.T.Y. conceived and designed the study. R.K. and M.A.I. conducted the experiment. S.Z.Z. and D.R.P. were responsible for experimental setup arrangements. R.K. and M.A.I. analyzed and revised the dataset. R.K. led the writing of the manuscript.

Funding: This research received no external funding.

Conflicts of Interest: “The authors declare no conflict of interest."

References

1. Keller, A. A.; McFerran, S.; Lazareva, A.; Suh, S. Global life cycle releases of engineered nanomaterials. *J. Nanoparticle Res.* **2013**, *15*, doi:10.1007/s11051-013-1692-4.
2. Handy, R. D.; Von Der Kammer, F.; Lead, J. R.; Hassellöv, M.; Owen, R.; Crane, M. The ecotoxicology and chemistry of manufactured nanoparticles. *Ecotoxicology* **2008**, *17*, 287–314, doi:10.1007/s10646-008-0199-8.
3. Xia, T.; Kovochich, M.; Liong, M.; Mädler, L.; Gilbert, B.; Shi, H.; Yeh, J. I.; Zink, J. I.; Nel, A. E. Comparison of the Mechanism of toxicity of Zinc and Cerium Oxide Nanoparticles Based on Dissolution and Oxidative Stress Properties. *Am. Chem. Soc. Nano* **2008**, *2*, 2121–2134, doi:10.1021/nn800511k.
4. Brunner, T. J.; Wick, P.; Manser, P.; Spohn, P.; Grass, R. N.; Limbach, L. K.; Bruinink, A.; Stark, W. J. In vitro cytotoxicity of oxide nanoparticles: Comparison to asbestos, silica, and the effect of particle solubility. *Environ. Sci. Technol.* **2006**, *40*, 4374–4381, doi:10.1021/es052069i.
5. Zhang, Y.; Chen, Y.; Westerhoff, P.; Hristovski, K.; Crittenden, J. C. Stability of commercial metal oxide nanoparticles in water. *Water Res.* **2008**, *42*, 2204–2212, doi:10.1016/j.watres.2007.11.036.
6. Baalousha, M. Aggregation and disaggregation of iron oxide nanoparticles: Influence of particle concentration, pH and natural organic matter. *Sci. Total Environ.* **2009**, *407*, 2093–2101, doi:10.1016/j.scitotenv.2008.11.022.
7. Majedi, S. M.; Kelly, B. C.; Lee, H. K. Combined effects of water temperature and chemistry on the environmental fate and behavior of nanosized zinc oxide. *Sci. Total Environ.* **2014**, *496*, 585–593, doi:10.1016/j.scitotenv.2014.07.082.
8. Degen, A.; Kosec, M. Effect of pH and impurities on the surface charge of zinc oxide in aqueous solution. *J. Eur. Ceram. Soc.* **2000**, *20*, 667–673.
9. Zhou, D.; Keller, A. A. Role of morphology in the aggregation kinetics of ZnO nanoparticles. *Water Res.* **2010**, *44*, 2948–2956, doi:10.1016/j.watres.2010.02.025.
10. Mudunkotuwa, I. A.; Rupasinghe, T.; Wu, C.-M.; Grassian, V. H. Dissolution of ZnO Nanoparticles at Circumneutral pH: A Study of Size Effects in the Presence and Absence of Citric Acid. *Langmuir* **2012**, *28*, 396–403, doi:10.1021/la203542x.
11. Liu, W. S.; Peng, Y. H.; Shiung, C. E.; Shih, Y. H. The effect of cations on the aggregation of commercial ZnO nanoparticle suspension. *J. Nanoparticle Res.* **2012**, *14*, doi:10.1007/s11051-012-1259-9.
12. Bian, S. W.; Mudunkotuwa, I. A.; Rupasinghe, T.; Grassian, V. H. Aggregation and dissolution of 4 nm ZnO nanoparticles in aqueous environments: Influence of pH, ionic strength, size, and adsorption of humic acid. *Langmuir* **2011**, *27*, 6059–6068, doi:10.1021/la200570n.
13. Van Hoecke, K.; De Schamphelaere, K. A. C.; Van Der Meeren, P.; Smagghe, G.; Janssen, C. R. Aggregation and ecotoxicity of CeO2 nanoparticles in synthetic and natural waters with variable pH, organic matter concentration and ionic strength. *Environ. Pollut.* **2011**, *159*, 970–976, doi:10.1016/j.envpol.2010.12.010.
14. Philippe, A.; Schaumann, G. E. Interactions of dissolved organic matter with natural and engineered inorganic colloids: A review. *Environ. Sci. Technol.* **2014**, *48*, 8946–8962, doi:10.1021/es502342r.
15. Zhu, M.; Wang, H.; Keller, A. A.; Wang, T.; Li, F. The effect of humic acid on the aggregation of titanium dioxide nanoparticles under different pH and ionic strengths. *Sci. Total Environ.* **2014**, *487*, 375–380, doi:10.1016/j.scitotenv.2014.04.036.
16. Keller, A. A.; Wang, H.; Zhou, D.; Lenihan, H. S.; Cherr, G.; Cardinale, B. J.; Miller, R.; Zhaoxia, J. I. Stability and aggregation of metal oxide nanoparticles in natural aqueous matrices. *Environ. Sci. Technol.* **2010**, *44*, 1962–1967, doi:10.1021/es902987d.
17. Li, X.; Lenhart, J. J.; Walker, H. W. Aggregation kinetics and dissolution of coated silver nanoparticles. *Langmuir* **2012**, *28*, 1095–1104, doi:10.1021/la202328n.
18. Zhang, Y.; Chen, Y.; Westerhoff, P.; Crittenden, J. Impact of natural organic matter and divalent cations on the stability of aqueous nanoparticles. *Water Res.* **2009**, *43*, 4249–4257, doi:10.1016/j.watres.2009.06.005.
19. Peng, C.; Shen, C.; Zheng, S.; Yang, W.; Hu, H.; Liu, J.; Shi, J. Transformation of CuO Nanoparticles in the Aquatic Environment: Influence of pH, Electrolytes and Natural Organic Matter. *Nanomaterials* **2017**, *7*, 326, doi:10.3390/nano7100326.
20. Peng, Y. H.; Tsai, Y. C.; Hsiung, C. E.; Lin, Y. H.; hsin Shih, Y. Influence of water chemistry on the environmental behaviors of commercial ZnO nanoparticles in various water and wastewater samples. *J. Hazard. Mater.* **2017**, *322*, 348–356, doi:10.1016/j.jhazmat.2016.10.003.

21. Khan, R.; Inam, M. A.; Zam, S. Z.; Park, D. R.; Yeom, I. T. Assessment of Key Environmental Factors Influencing the Sedimentation and Aggregation Behavior of Zinc Oxide Nanoparticles in Aquatic Environment. **2018**, 1–18, doi:10.3390/w10050660.
22. He, G.; Chen, R.; Lu, S.; Jiang, C.; Liu, H.; Wang, C.; He, G.; Chen, R.; Lu, S.; Jiang, C.; Liu, H.; Wang, C.; Liu, H.; Wang, C. Dominating Role of Ionic Strength in the Sedimentation of Nano-TiO_2 in Aquatic Environments. *J. Nanomater.* **2015**, *2015*, 1–10, doi:10.1155/2015/851928.
23. Dong, Y.; Li, X.; Huang, Y.; Wang, H.; Li, F. Coagulation and dissolution of zinc oxide nanoparticles in the presence of humic acid under different pH values. *Environ. Eng. Sci.* **2016**, *33*, 347–353.
24. Kato, H.; Fujita, K.; Horie, M.; Suzuki, M.; Nakamura, A.; Endoh, S.; Yoshida, Y.; Iwahashi, H.; Takahashi, K.; Kinugasa, S. Dispersion characteristics of various metal oxide secondary nanoparticles in culture medium for in vitro toxicology assessment. *Toxicol. Vitr.* **2010**, *24*, 1009–1018.
25. Smoluchowski, M. In Graetz, L (Ed.) Handbuch der Elektrizitat und Magnetisums 1914.
26. Phadke, M. 5 *Uauty Engineering Using Robust Design*; ISBN 0137451679.
27. CBC, R.; HL, Q. Advanced oxidation processes for wastewater treatment: Optimization of UV/H2O2 process through a statistical technique. *Chem. Eng. Sci.* **2005**, *60*, 5305–5311, doi:10.1016/j.ces.2005.03.065.
28. Lan, W. G.; Wongt, M. K.; Chen, N.; Sin, Y. M. Analyst, April 1995, Vol. 120 1115. **1995**, *120*, 1115–1124.